Letter to the Editor

Med Ultrason 2023, Vol. 25, no. 2, 236-245

Ultrasonography-guided botulinum toxin injection for lumbrical muscle spasticity in a hemiplegic patient

Emre Ata[1], Mehmet Akif Güler[1], Emre Adıgüzel[2]

[1]Department of Physical Medicine and Rehabilitation, Sultan II. Abdulhamit Han Training and Research Hospital, Istanbul, [2]University of Health Sciences Turkiye, Ankara City Hospital, Physical Medicine and Rehabilitation Hospital, Ankara, Turkiye

To the Editor,

Spasticity can cause hand hygiene problems, deformities and macerations, especially in hemiplegic patients. Ultrasonography-guided botulinum toxin injection is an invasive procedure frequently used in the treatment of spasticity in hemiplegic patients. With the widespread use of ultrasonography in recent years, it has facilitated the application of intramuscular botulinum injections [1,2]. Lumbrical muscles are a group of 4 small muscles that provide flexion of the metacarpophalangeal joints and cause impairment in hand functions due to spasticity in patients with hemiplegia. Ultrasonography-guided botulinum toxin injection of these muscles has not been shown before. The purpose of this article is to describe ultrasonography-guided botulinum muscle injection of lumbrical muscles for the treatment of spasticity in a patient with spastic hemiplegia.

The patient's metacarpophalangeal joint should be placed at 90º flexion. For easy application, the practitioner can grasp 4 fingers with their hand. After the position is achieved, the transducer is placed in the interphalangeal space on the dorsum of the hand as shown in figure 1A. The lumbricals can be reached from both the palmar surface and the dorsal surface. It is located just above/below the dorsal interosseous muscles. Superficialis and profundus muscle tendons are seen in the lateral parts. The muscles seen in this range are as seen above and below. A long 27 Gauge dental tip can be used as a needle tip. The upper pole of the interdigital web should be aimed as the entry point of the needle. The needle is advanced so that it is parallel to the ground. Botulinum toxin injection using appropriate dosage can be applied to the lumbrical muscles in every 3 interphalangeal spaces and 1st lumbrical muscle.

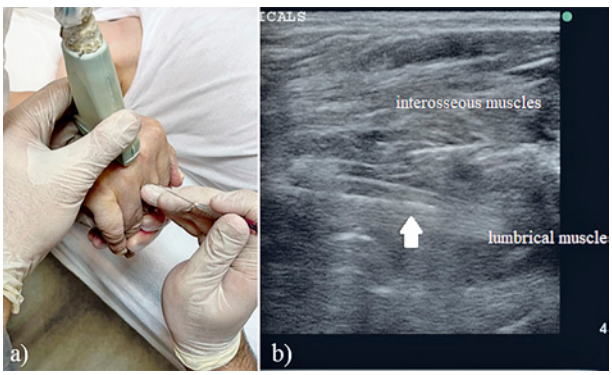

Fig 1. a) The hand should be positioned as the metacarpophalangeal joint at 90º of flexion. The ultrasound probe is placed longitudinally on the dorsum of the patient's hand. One end of the ultrasound probe should be at the level of the metacarpophalangeal joint. The entry point of the needle should be in the intermetacarpal area, just above the interdigital web, parallel to the ultrasound probe; b) The lumbrical muscles are located just below the dorsal interosseous muscles. Since the needle is parallel to the ultrasound transducer, it can be easily seen (arrows). In this way, an easy and effective application can be performed while protecting the digital artery.

References

1. Walker HW, Lee MY, Bahroo LB, et al. Botulinum toxin injection techniques for the management of adult spasticity. PM&R. 2015;7:417-427.
2. Alter KE. High-frequency ultrasound guidance for neurotoxin injections. Phys Med Rehabil Clin N Am. 2010;21: 607-630.

Received 17.03.2023 Accepted 22.04.2023
Med Ultrason
2023, Vol. 25, No 2, 236, DOI: 10.11152/mu-4105,
Corresponding author: Mehmet Akif Güler
Department of Physical Medicine and Rehabilitation, Sultan II Abdulhamit Han Training and Research Hospital, Istanbul, Turkey
E-amil: makifguler89@gmail.com

The role of lung ultrasonography in the SARS-CoV-2 vaccines and variants era: a case report

Javier González Cepeda[1], Ana Luisa Esteves[2], Raquel Marín-Baselga[1], Yale Tung-Chen[1]

[1]Department of Internal Medicine. Hospital Universitario La Paz (Madrid, Spain), [2]Internal Medicine Department, Hospital de Egas Moniz, Centro Hospitalar de Lisboa Ocidental, Lisbon, Portugal

To the Editor,

Constantly emerging SARS-CoV-2 variants are exhibiting heterogenous behaviour regarding immune invasion, transmissibility, and clinical manifestations. Clinically, an Omicron infection is associated with a lower risk of complications [1]. Furthermore, investigation revealed that Omicron is totally or partially resistant to most SARS-CoV-2 neutralizing antibodies, decreasing vaccine efficacy against this variant [2].

In this report, we present the case of a 37-year-old man, non-smoker, without further pre-existing conditions besides a COVID-19 infection in March of 2020 [3]. At the time of infection, daily ultrasound evaluation exhibited anomalies compatible with bilateral pulmonary affection, with the appearance of pleural effusion, pleural line irregularities, consolidations, and confluent B lines (fig 1a), which normalized three weeks after the negative PCR test. He was vaccinated with two doses of BioNTech (Pfizer) and one dose of Moderna. In June of 2022, he reported odynophagia, dry cough, intense asthenia, and fever (maximum 38.2 ºC), presenting a positive test for SARS-CoV-2 variant Omicron BA.4/5. He would occasionally present episodes of asymptomatic desaturation (from 98% to 93%), which triggered a daily ultrasound evaluation that was performed following a 12-zone protocol using a portable device - Butterfly IQ (Butterfly Network, Guilford, CT, EE. UU.). No abnormalities were found (figure 1b). Clinically the patient received only symptomatic treatment. The following week, he went back to work without any further occurrences.

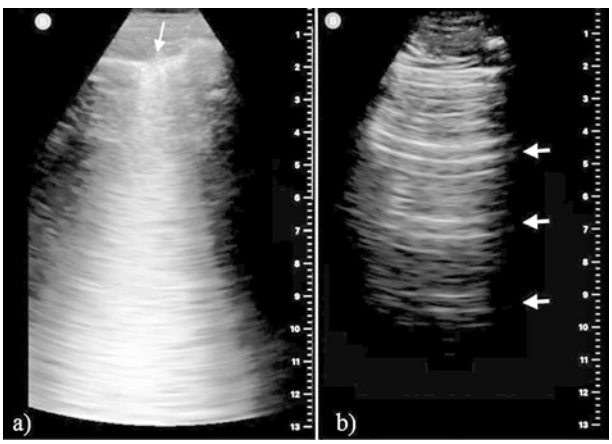

Fig 1. Lung ultrasound performed with a portable device in the same patient in March of 2020 (a) and June of 2022 and in (b): a) Confluent B line pattern (white arrow); b) Normal A line pattern (horizontal lines, white arrow).

In the actual context of highly transmissible Omicron and its subvariants, with a diminished vaccine efficacy and less involvement of the lower respiratory tract, most patients present with mild symptoms and do not require hospitalization, as shown in this case report. Nevertheless, pulmonary imaging is fundamental for diagnostic and treatment guidance. In this different scenario, lung ultrasound stands out as an accessible and extensively demonstrated diagnostic tool [4]. Additionally, in non-hospital settings and in areas with limited resources, it becomes even more valuable. Its value is probably extrapolated for SARS-CoV-2 subvariants. However, the relative scarcity of physicians qualified to perform lung ultrasound made the use of this method difficult in large scale.

Received 29.01.2023 Accepted 22.04.2023
Med Ultrason
2023, Vol. 25, No 2, 237-238, DOI: 10.11152/mu-4053,
Corresponding author: Yale Tung Chen MD
Department of Internal Medicine,
Hospital Universitario La Paz (Madrid, Spain)
Madrid, Spain
E-mail: yale.tung.chen@gmail.com

References

1. Sun C, Xie C, Bu GL, Zhong LY, Zeng MS. Molecular characteristics, immune evasion, and impact of SARS-CoV-2 variants. Signal Transduct Target Ther 2022;7:202.

2. Marta RA, Nakamura GEK, de Matos Aquino B, et al. COVID-19 Vaccines: Update of the vaccines in use and under development. Vacunas 2022;23:S88-S102.
3. Tung-Chen Y. Lung ultrasound in the monitoring of COVID-19 infection. Clin Med (Lond) 2020;20:e62-e65.
4. Hernández-Píriz A, Tung-Chen Y, Jiménez-Virumbrales D, et al. Usefulness of lung ultrasound in the early identification of severe COVID-19: results from a prospective study. Med Ultrason 2022;24:146-152.

Diagnosing metatarsal chip fractures with ultrasound: faster and better

Yu-Hsuan Chen[1], Chueh-Hung Wu[2], Levent Özçakar[3]

[1]Department of Education, National Taiwan University Hospital, Taipei, Taiwan, [2]Department of Physical Medicine and Rehabilitation, National Taiwan University Hospital, College of Medicine, National Taiwan University, Taipei, Taiwan, [3]Department of Physical and Rehabilitation Medicine, Hacettepe University Medical School, Ankara, Turkey

To the Editor,

A healthy 32-year-old male visited our emergency department after a traffic accident involving two scooters. Abrasion wounds along with swelling, pain, and limited range of motion over his right ankle were noted. X-rays of the pelvis, right hand, knee, and ankle were normal. The patient was therefore discharged with advice to apply ice and rest.

Persistent swelling and pain (visual analogue scale of 4 out of 10) were noted one week after the accident. Upon his visit to the orthopedics clinic, another X-ray was performed and showed no obvious fracture/dislocation. Persistent pain for another week prompted him to visit our rehabilitation clinic. Ultrasonography revealed cortical disruption at the base of the 3rd metatarsal bone and a chip fracture was highly suspected (fig 1A). Computed tomography (CT) scan of the right foot confirmed the diagnosis of fractured 3rd metatarsal bone and lateral cuneiform (fig 1B,C). He was then advised to prevent from bearing weight with an air splint for 8-12 weeks.

Metatarsal fractures comprise approximately 35% of all foot fractures whereby isolated cuneiform fractures are rare [1]. They are usually associated with serial metatarsal fractures resulting from high-energy injuries. Patients can present with pain, swelling and inability to bear weight or walk. Diagnosis is usually made with plain films of the foot in the anteroposterior, 45º oblique, and lateral projections. However, the sensitivity of these views is challenged clinically as fractures often/initially go undetected. CT scans and magnetic resonance imag-

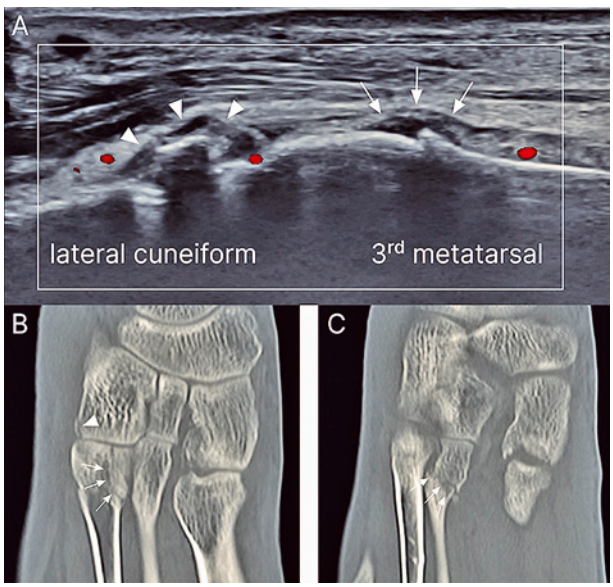

Fig 1. A) Longitudinal ultrasound image shows cortical disruption and hypoechoic periosteal thickening associated with mild hyperemia of the 3rd metatarsal bone (arrows) and the lateral cuneiform (arrowheads); B and C) CT scans in axial plane reveal the fractured 3rd metatarsal bone (arrows) and lateral cuneiform (arrowheads).

Received 21.01.2023 Accepted 30.03.2023
Med Ultrason
2023, Vol. 25, No 2, 238-239, DOI: 10.11152/mu-4040,
Corresponding author: Chueh-Hung Wu, MD, PhD
7 Chan-Shan South Road,
100, Taipei, Taiwan
Phone: 886-2-23123456-66473
E-mail: b88401062@ntu.edu.tw
nojred@gmail.com

ing are the most sensitive tools, but they are unavailable in many settings. On the other hand, point-of-care ultrasonography facilitates visualization of tiny lesions [2]. As regards foot and ankle fractures, its sensitivity ranges from 87.3 to 100% and it therefore serves as a cost-effective screening tool [3].

Treatment for undisplaced metatarsal and tarsometatarsal fractures is immobilization for 3-6 weeks, with protective measures ranging from adhesive strapping to non-weight-bearing casts [1]. Displaced fractures that alter weight distribution or open fractures require surgical treatment. An early diagnosis and appropriate treatment can prevent post-injury complications, such as overload of adjacent metatarsals and deformities. In short, for a patient with persistent pain after a traumatic event, ultrasonography should be performed to detect chip fractures even if plain films fail to show them.

References

1. Samaila EM, Ditta A, Negri S, Leigheb M, Colo G, Magnan B. Central metatarsal fractures: a review and current concepts. Acta Biomed 2020;91:36-46.
2. Wei KC, Wu CH, Ozcakar L. Ultrasound Imaging and Guidance in the Diagnosis and Hydrodissection of Superficial Radial Nerve Entrapment After Fracture Surgery. Pain Med 2020;21:2001-2002.
3. Champagne N, Eadie L, Regan L, Wilson P. The effectiveness of ultrasound in the detection of fractures in adults with suspected upper or lower limb injury: a systematic review and subgroup meta-analysis. BMC Emerg Med 2019;19:17.

Ultrasound findings of Castleman's disease of the parotid gland

Lan Ding, Xiaoping Chen, Xiuxiu Zhu

Department of Ultrasound, Deqing County Hospital of Traditional Chinese Medicine, Deqing, Zhejiang, P.R. China

To the Editor,

A 38-year-old male was admitted to the hospital due to a mass under the left ear; there was no tenderness or erythema on clinical exam. Ultrasound revealed a hypoechoic mass in the left parotid gland (approximately 25×15 mm) with clear boundaries and uniform internal echo. Color Doppler flow imaging (CDFI) showed a slightly rich blood flow signal. The hypoechoic mass in the left parotid gland was considered as a probable adenolymphoma (fig 1a,b). A nodular, slightly low-density shadow (2.5×1.6 cm) with clear boundaries was found in the left parotid gland via computed tomography. Enhancement of the arterial phase was obvious in the enhanced scan, and a vascular welt sign was observed. This enhancement was slightly reduced in the venous phase.

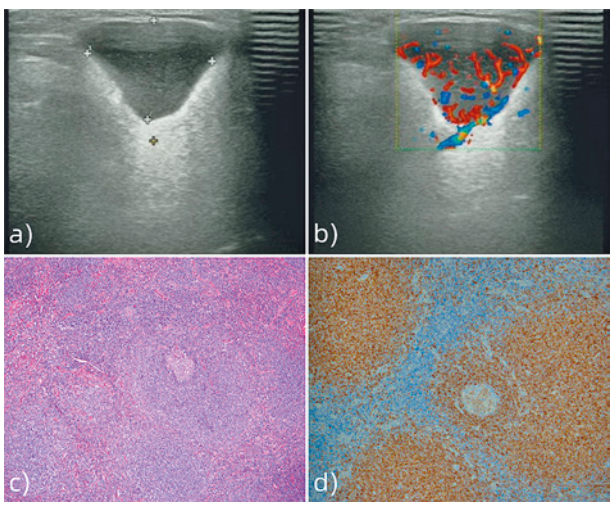

Fig 1. a) A hypoechoic mass is seen in the left parotid gland; b) CDFI shows a slightly rich blood flow signal; c) Microscopy reveals lymphoid hyperplasia with a large number of hyaline vessels (hematoxylin and eosin stain, 50× magnification); d) Immunohistochemistry reveals CD79a-positive lymphoid tissues (100× magnification).

Received 23.02.2023 Accepted 22.04.2023
Med Ultrason
2023, Vol. 25, No 2, 239-240, DOI: 10.11152/mu-4079,
Corresponding author: Lan Ding
Department of Ultrasound, Deqing County Hospital of Traditional Chinese Medicine, Deqing, Zhejiang, 313216, P. R. China
Phone: +86 13757266731
E-mail: 522978688@qq.com

Partial left parotid gland superficial lobe resection was performed. Postoperative pathology revealed Castleman's disease (CD) of the hyaline vascular subtype (fig 1c). Immunohistochemical staining revealed the following: CD3(–), CD5(–), CD20(+), CD79a(+), cyclinD1(–), and Ki-67 positivity of 10% (fig 1d).

CD is a rare lymphoproliferative disease, also known as giant lymph node hyperplasia. Clinically, it is classified as unicentric CD (UCD) or multicentric CD (MCD) based on number of lymph nodes affected in a region [1]. Parotid gland CD often presents as an asymptomatic painless mass, making diagnosis challenging. High-frequency ultrasound has the advantages of high resolution and being non-invasive, economical, and simple; therefore, it is the preferred method for examining parotid gland masses. In ultrasound exploration of the parotid region, if solid masses have clear edges and intermittent short linear hyperechoes, as well as observable rich blood supply are visualized, parotid gland CD cannot be excluded. Further, the scan scope should be expanded, and a multi-site scan should determine the presence of single- or multiple-site lesions. A final diagnosis of CD depends on pathological findings.

Surgical resection is the preferred treatment for UCD and is associated with a good prognosis. Currently, MCD treatment standards have not been clarified, prognosis is poor, and patients require long-term follow-up [2].

References

1. Wu D, Lim MS, Jaffe ES. Pathology of Castleman disease. Hematol Oncol Clin North Am 2018;32:37-52.
2. Wang W, Medeiros LJ. Castleman disease. Surg Pathol Clin 2019;12:849-863.

"Reverse" curtain sign for diagnosis of pneumothorax

Chun-Ta Huang, Sheng-Yuan Ruan

Department of Internal Medicine, National Taiwan University Hospital, Taipei, Taiwan

To the Editor,

A 77-year-old woman with history of gallstones presented to the emergency department with fever and abdominal pain. Physical examination revealed a temperature of 38.6°C, tenderness over the right upper quadrant of the abdomen, and the presence of Murphy's sign. Computed tomography showed a distended gallbladder with multiple stones and pericholecystic fluid. With a diagnosis of acute cholecystitis, percutaneous transhepatic gallbladder drainage was performed. Ultrasound on admission displayed a normal curtain sign (fig 1a, Video 1 on the journal site), i.e., dynamic rostral-to-caudal movement of the lung curtain and non-visualization of the lateral hemidiaphragm in the respiratory cycle. During the treatment course, the patient developed right pleural effusion and had a failed diagnostic thoracentesis with dry taps. The next day, the patient experienced respiratory distress and required oxygen. Ultrasound revealed a "reverse" curtain sign (fig 1b, video 2 on the journal site), i.e., appearance of the air curtain from the caudal to rostral side of the right hemithorax. The finding suggests the presence of intrathoracic free air or pneumothorax around the right costophrenic recess. Iatrogenic pneumothorax was diagnosed, and the patient underwent right tube thoracostomy and made an uneventful recovery.

Pneumothorax is iatrogenic when its development is associated with an invasive medical procedure. The prevalence of iatrogenic pneumothorax likely varies with procedures performed, underlying lung disease, and operator experience [1]. In a large-scale study, its prevalence was approximately 1.5% [1], with the leading two procedures, central venous catheterization, and thoracentesis. Chest ultrasound is superior to conventional chest radiography for the diagnosis of pneumothorax given its bedside availability, radiation-free property, capability of

Received 18.02.2023 Accepted 22.04.2023
Med Ultrason
2023, Vol. 25, No 2, 240-241, DOI: 10.11152/mu-4074,
Corresponding author: Chun-Ta Huang, MD
Department of Internal Medicine,
National Taiwan University Hospital,
7, Chung-Shan South Road, Taipei, Taiwan
Phone/Fax: 886-2-23562905
886-2-23582867
E-mail: huangct@ntu.edu.tw

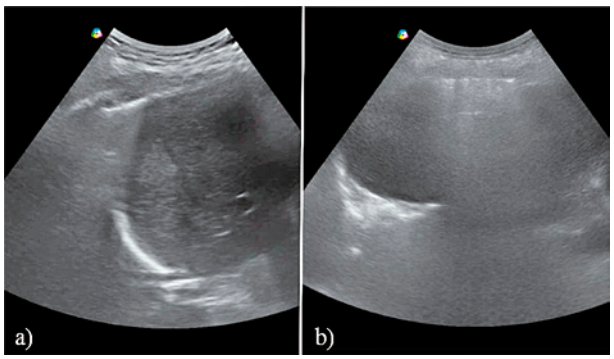

Fig 1. a) Normal right costophrenic angle. Chest ultrasound shows a normally aerated lung obscuring the right costophrenic recess. b) Abnormal right costophrenic angle. Chest ultrasound shows the presence of a right pleural effusion and free air overlying the right hemidiaphragm and liver.

guiding therapeutic interventions, and higher diagnostic sensitivity [2]. A normal curtain sign implies a fully aerated lung at the costophrenic recess [3]; however, a "reverse" curtain sign, i.e., abnormal air curtain moving in a caudal-to-rostral way, is suggestive of pneumothorax around the costophrenic angle.

References

1. Celik B, Sahin E, Nadir A, Kaptanoglu M. Iatrogenic pneumothorax: etiology, incidence and risk factors. Thorac Cardiovasc Surg 2009;57:286-290.
2. Alrajhi K, Woo MY, Vaillancourt C. Test characteristics of ultrasonography for the detection of pneumothorax: a systematic review and meta-analysis. Chest 2012;141:703-708.
3. Lee FCY. The Curtain Sign in Lung Ultrasound. J Med Ultrasound 2017;25:101-104.

Semimembranosus muscle tear masquerading as a hypervascular tumor: ultrasonographic differential diagnosis for gluteal pain syndrome

Wei-Ting Wu[1,2], Kamal Mezian[3], Vincenzo Ricci[4], Ke-Vin Chang[1,2,5], Levent Özçakar[6]

[1]Department of Physical Medicine and Rehabilitation, National Taiwan University Hospital, Bei-Hu Branch, Taipei, Taiwan, [2]Department of Physical Medicine and Rehabilitation, National Taiwan University College of Medicine, Taipei, Taiwan, [3]Department of Rehabilitation Medicine, First Faculty of Medicine and General University Hospital, Charles University in Prague, Prague, Czech, [4]Physical and Rehabilitation Medicine Unit, Luigi Sacco University Hospital, ASST Fatebenefratelli-Sacco, Milan, Italy, [5]Center for Regional Anesthesia and Pain Medicine, Wang-Fang Hospital, Taipei Medical University, Taipei, Taiwan, [6]Department of Physical and Rehabilitation Medicine, Hacettepe University Medical School, Ankara, Turkey

To the Editor,

During speed walking three months ago, a 32-year-old female had experienced a sudden onset of right inferior gluteal pain which had worsened and started to cause limping. She had sought treatment at a rehabilitation clinic where she had initially been diagnosed with deep gluteal pain syndrome. However, despite medication and physical therapy, her pain persisted. Using a high-end ultrasound (US) machine equipped with a 5-13 MHz transducer, a circular mass with a hypoechoic rim and a hyperechoic core located medial to the proximal biceps femoris muscle in the axial plane was seen (fig 1a). In the sagittal plane, the mass was found in the middle of the semitendinosus muscle, over the semimembranosus tendon (fig 1b). Doppler US imaging showed petechial vascularity in the mass (fig 1c). Subsequent magnetic resonance imaging revealed fluid surrounding the retracted proximal semitendinosus muscle (fig 1d), leading to a diagnosis of partial tear in the semimembranosus muscle. The patient received 25% dextrose injections (10 mL) twice and experienced complete pain relief at the two-month post-injection follow-up.

Received 01.04.2023 Accepted 23.04.2023
Med Ultrason
2023, Vol. 25, No 2, 241-242, DOI: 10.11152/mu-4115,
Corresponding author: Ke-Vin Chang
Department of Physical Medicine and Rehabilitation, National Taiwan University Hospital Bei-Hu Branch, No. 87, Nei-Jiang Rd., Wan-Hwa District, Taipei 108, Taiwan
E-mail: kvchang011@gmail.com
Phone: +886223717101-5309

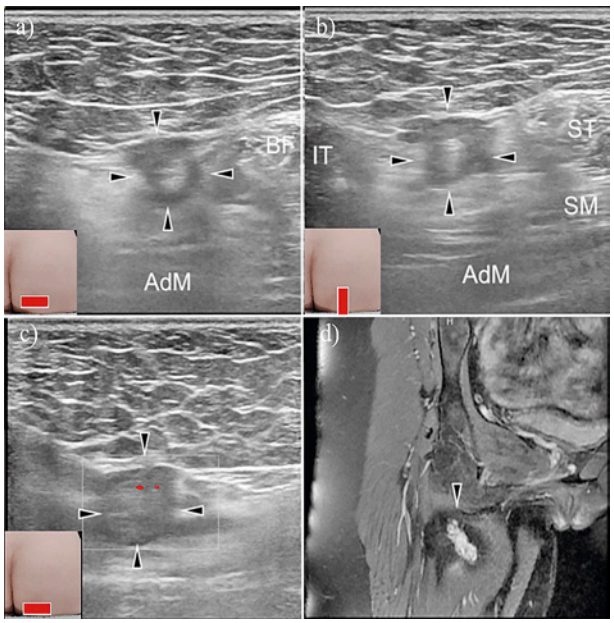

Fig 1. a) Axial imaging shows a circular mass *(black arrows)* with hypoechoic rim and hyperechoic core; b) Sagittal imaging shows the mass inside the semitendinosus muscle; c) Doppler ultrasound shows intra-lesional vascularity; d) T2-weighted coronal magnetic resonance imaging reveals fluid around the retracted muscle. BF, biceps femoris; ST, semitendinosus muscle; SM, semimembranosus muscle; IT, ischial tuberosity; AdM, adductor magnus.

US examination is a valuable tool for assessing muscle quality and quantity [1], particularly in cases of traumatic muscle injury [2]. Peetrons et al. [3] proposed the most widely used grading system as Grade 1 (involving <5% of the target muscle), Grade 2 (involving >5% of the target muscle with some connected muscle fibers), or Grade 3 (a complete rupture with significant retraction). In our case, more than 5% of the semitendinosus muscle was torn, but there were still connected muscle fibers i.e. Grade 2 traumatic muscle injury. Regenerative injection therapies such as platelet-rich plasma or high-concentration dextrose may be beneficial for this type of injury [4]. The myotendinous junction was the site of the lesion, indicating a likely strain mechanism (overstretching of a shortened muscle). On US, the hypoechoic rim was caused by exudation of blood, while the hyperechoic core represented the retracted muscle fibers. Due to the time period (>3 months) between the injury and the US exam, neovascularization had occurred i.e., peripheral hypervascularity that caused the lesion to appear like a hypervascular mass.

Acknowledgment: The study was made possible by 1) the research funding of the Community and Geriatric Medicine Research Center, National Taiwan University Hospital, Bei-Hu Branch, Taipei, Taiwan; 2) Ministry of Science and Technology (MOST 106-2314-B-002-180-MY3, 109-2314-B-002-114-MY3 and 109-2314-B-002-127); and 3) Taiwan Society of Ultrasound in Medicine.

References

1. Chang KV, Wu WT, Huang KC, Jan WH, Han DS. Limb muscle quality and quantity in elderly adults with dynapenia but not sarcopenia: An ultrasound imaging study. Exp Gerontol 2018;108:54-61
2. Chang KV, Wu WT, Özçakar L.Ultrasound Imaging and Rehabilitation of Muscle Disorders: Part 1. Traumatic Injuries. Am J Phys Med Rehabil 98:1133-1141
3. Peetrons P (2002) Ultrasound of muscles. Eur Radiol 2019;12:35-43
4. Ilker S, Aydan O.Features and Clinical Effectiveness of the Regenerative Injection Treatments: Prolotherapy and Platelet-Rich Plasma for Musculoskeletal Pain Management. In: Marco C (ed) From Conventional to Innovative Approaches for Pain Treatment. IntechOpen, Rijeka, 2019

Ultrasound and pathology findings of adenomyoepithelioma in the breast: a case report

Xiaowei Zhang[1], Kangbin Wu[2], Saiping Fu[2]

[1]Department of Pathology, [2]Department of Breast Disease Treatment Center, Affiliated Dongyang Hospital of Wenzhou Medical University, Dongyang, Zhejiang, P. R. China

To the Editor

A 77-year-old female patient was admitted because of a mass in her right breast. Ultrasound examination revealed a low-echo nodule of the size 25×26×14 mm at 10 o'clock in the right breast, with clear boundaries, multiple lobules, and uniform internal echoes. A blood flow signal was observed on color Doppler flow imaging. Hypoechoic nodules in the right breast were BIRADS category 4A. Multiple lymph nodes were detected in the bilateral axilla (fig 1a,b).

A right breast mass resection was performed. A postoperative pathological examination led to a diagnosis of adenomyoepithelioma (AME) with negative resection margins. Immunohistochemical staining yielded the following results: estrogen receptor (moderate +, 10%), progesterone receptor (-), human epidermal growth factor receptor 2 (0), cytokeratin 5/6 (+), p63 (-), calponin (+), S-100 (+), synaptophysin (-), chromogranin A (-), cluster differentiation 56 (-), smooth muscle actin (-), desmin (-), cytokeratin (AE1 /AE3) (+), vimentin (+), and Ki-67 (+, 3%) (fig 1c,d). No recurrence or distant metastasis was observed after 13 months.

AME commonly presents as an isolated palpable painless nodule located in the periphery of the breast, occasionally subareolar or in the central region of the breast. In a few patients, it may be accompanied by nipple discharge [1]. The AME imaging findings showed no specificity. Ultrasonography revealed an irregular or oval mass with low echogenicity and lobulation. Breast molybdenum targets appear as round or lobulated dense masses with indistinct borders and may be accompanied by calcification. Preoperative diagnosis of AME is difficult and depends on pathological examination.

AME is usually a benign tumor, and local recurrence can occur in patients with incomplete resection. In some cases, malignant transformation of epithelial or myoepithelial components occurs [2]. In our case, the patient had a large tumor removed via right breast segment resection, with extended margins of >1.0 cm. No recurrence or distant metastasis was observed 13 months postoperatively.

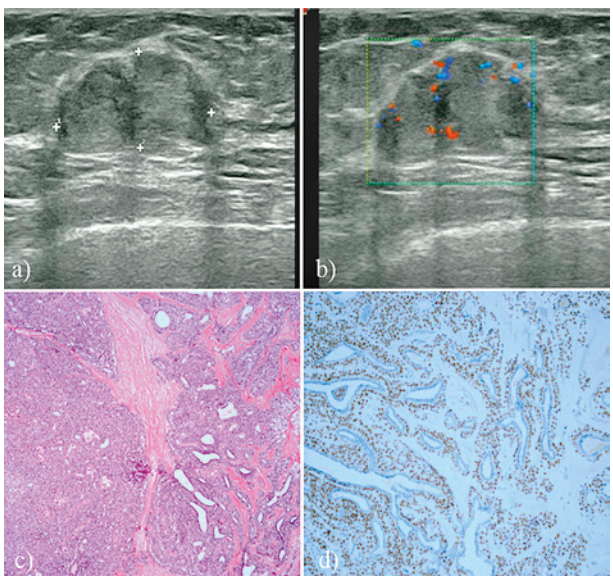

Fig 1. a) Hypoechoic nodule in the right breast with clear boundaries; b) Blood flow signal on Color Doppler flow imaging; c) Tumor appearing nodular on hematoxylin and eosin (HE) staining (×50); d) Immunohistochemical analysis of myoepithelial cells revealing expression of P63 (immunohistochemistry ×100).

Received 04.01.2023 Accepted 30.03.2023
Med Ultrason
2023, Vol. 25, No 2, 243-244, DOI: 10.11152/mu-4034,
Corresponding author: Saiping Fu
Department of Breast Disease Treatment Center,
Affiliated Dongyang Hospital of Wenzhou Medical University,
Dongyang, Zhejiang,
322100, P. R. China
Phone/fax: +86 13868931153
+86 057986856211
E-mail: fusaiping202212@163.com

References

1. Rakha E, Tan PH, Ellis I, Quinn C. Adenomyoepithelioma of the breast: a proposal for classification. Histopathology 2021;79:465-479.
2. Kakkar A, Jangra K, Kumar N, Sharma MC, Mathur SR, Deo SS. Epithelial-myoepithelial carcinoma of the breast: A rare type of malignant adenomyoepithelioma. Breast J 2019;25:1273-1275.

An asymptomatic idiopathic giant right atrial aneurysm. A case report

Xuanshou Xu[1], Yaqun Tang[1], Cixiang Wen[2], Heng Zhang[1]

[1]Department of Ultrasound, Zhuhai People's Hospital (Zhuhai hospital affiliated with Jinan University), [2]Department of Ultrasound, Zhuhai Hospital of integrated Traditional Chinese and Western Medicine, Zhuhai, China

To the Editor,

A 4-year-old male patient, with no prior medical history, presenting with sudden pain under the xiphoid process for 5 hours, was admitted. The cardiopulmonary physical examination and related biochemical indexes were normal.

The transthoracic echocardiography showed that a huge aneurysm-like structure originated from the lateral wall of the right atrium (fig 1a), about 60x40 mm in size. The right ventricle was extruded and deformed by the aneurysm-like structure. There was no thrombosis in the structure and no sign of anomalous pulmonary venous drainage. We also found a defect of about 12 mm in the middle of the atrial septum (fig 1b). It appears that a 'sail-like' structure can be seen in the anterior lobe of the tricuspid valve during continuous scanning of the apical four-chamber view. At first, it was regarded as a broad, lengthy anterior lobe of the tricuspid valve, explaining the previous interpretation as Ebstein's anomaly. Similar misdiagnosis has been reported [1-2]. But the above 'sail-like' structure did not detect the valve-like open and closed motion during the whole cardiac cycle under the careful observation. Moreover, the position and development of the three tricuspid valves were not abnormal and the above-mentioned 'sail-like' structure was part of the wall of the dilated atrial aneurysm by multi-section detection. According to the above imaging signs, an idiopathic right atrial aneurysm (RAA) was initially diagnosed, surgical treatment was recommended, and the huge atrial aneurysm was confirmed operatively (fig 1c). The pathology showed that the fibrous capsule wall was covered with flat cells, surrounded by partially degenerated rhabdomyolysis tissue, with local arrangement disorder and edema (fig 1d). The patient has no postoperative discomfort and receives echocardiographic follow-up.

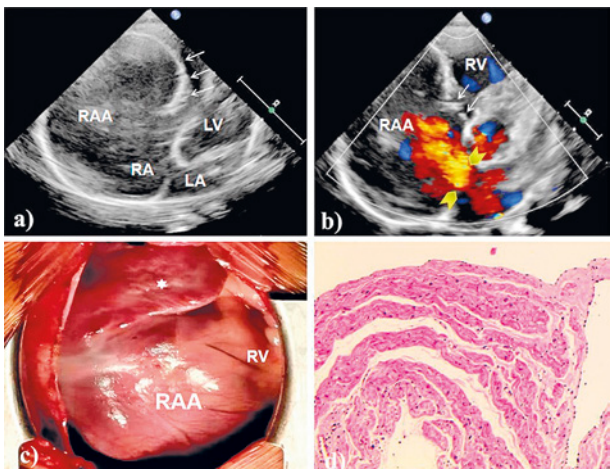

Fig 1. a) A massive RAA and its wall structure are shown by two-dimensional ultrasonography; b) Color doppler showed red septal blood flow at the interruption of the atrial septum, showing left-to-right shunt; c) The giant RAA occupied most of the operative field; d) The histopathologic of the right atrial aneurysm. RA: right atrium, RAA: right atrial aneurysm, RV: right ventricle, LA: left atrium, LV: left ventricle, tiny arrow: Tricuspid valve, wide arrow: Atrial septal defect, * Right atrial appendage

Congenital RAA is a rare congenital heart disease, which was defined as disproportionately larger right atrial enlargement than other cardiac cavities and exclud-

Received 09.01.2023 Accepted 31.03.2023
Med Ultrason
2023, Vol. 25, No 2, 244-245, DOI: 10.11152/mu-4039,
Corresponding author: Heng Zhang
Department of Ultrasound, Zhuhai People's Hospital (Zhuhai Hospital Affiliated to Jinan University), Zhuhai 519000, China,
E-mail: zh2157828@126.com

ing all known cardiovascular lesions [3]. RAA are rare, vary in location and imaging features, and knowledge of the sonographic features that may be present will give the sonographer the confidence to accurately diagnose it.

In conclusion, transthoracic echocardiography can determine the location and the adjacent structure of the atrial aneurysm. Besides, the valve activity and right ventricular function can also be evaluated. It conveys high clinical value in the diagnosis, preoperative evaluation and postoperative follow-up of the atrial aneurysm.

References

1. Klisiewicz A, Szymański P, Rózański J, Hoffman P. Giant congenital aneurysm of the right atrium: echocardiographic diagnosis and surgical management. J Am Soc Echocardiogr 2004;17:286-287.
2. Morrow AG, Behrendt DM. Congenital aneurysm (diverticulum) of the right atrium: clinical manifestations and results of operative treatment. Circulation 1968;38:124-128.
3. Sumner RG, Phillips JH, Jacoby WJ, Tucker DH. Idiopathic enlargement of the right atrium. Circulation 1965;32:985-991.